

Continuum and Symmetry-Conserving Effects in Drip-line Nuclei Using Finite-range Forces

N. Schunck^{1,2} and J. L. Egidio¹

¹*Departamento de Física Teórica, Universidad Autónoma de Madrid 28 049 Cantoblanco, Madrid, Spain*

²*University of Tennessee, Physics Division, 401 Nielsen Physics, Knoxville, TN 37996, USA
Oak Ridge National Laboratory, Bldg. 6025, MS6373, P.O. 6008, Oak Ridge, TN-37831, USA*

(Dated: August 17, 2021)

We report the first calculations of nuclear properties near the drip-lines using the spherical Hartree-Fock-Bogoliubov mean-field theory with a finite-range force supplemented by continuum and particle number projection effects. Calculations were carried out in a basis made of the eigenstates of a Woods-Saxon potential computed in a box, thereby guaranteeing that continuum effects were properly taken into account. Projection of the self-consistent solutions on good particle number was carried out after variation, and an approximation of the variation after projection result was used. We give the position of the drip-lines and examine neutron densities in neutron-rich nuclei. We discuss the sensitivity of nuclear observables upon continuum and particle-number restoration effects.

PACS numbers: PACS numbers: 21.10.Dr, 21.10.Gv, 21.10.Re, 21.30.Fe, 21.60.Ev, 21.60.Jz

One of the main challenges in contemporary nuclear structure is to describe nuclei far from the valley of stability. New radioactive ion beam facilities are under intense development and when in full exploitation will considerably increase the wealth of experimental data available [1]. From a theoretical point of view, neutron-rich or -deficient nuclei present two major challenges. Firstly, these nuclei are weakly-bound, and it is expected that the influence of the continuum of energy will significantly alter many nuclear properties [2]. However, the extent to which these properties will change due to the presence of the continuum is not so clear. Secondly both the nuclear mean-field theory and the nuclear shell model rely on effective interactions whose parameters were mostly adjusted on data in stable nuclei. The reliability and the robustness of these parametrizations under extreme isospin ratios must be questioned, and nuclei far from stability thus present us with a unique test-ground [1, 2].

Much effort was devoted in the recent years to the study of weakly-bound nuclei, and the development of the corresponding appropriate methods, within the framework of the non-relativistic mean-field theory with Skyrme interactions [3, 4, 5], relativistic mean-field [6] and the nuclear shell model [7]. In mean-field approaches, it was recognized early that the stability of very neutron-rich nuclei is caused to a great extent by pairing correlations, and that a fully self-consistent treatment of the latter in the Hartree-Fock-Bogoliubov formalism is required [3]. In the case of the Skyrme mean-field the zero-range of the interaction leads to the well-known divergence problem in the pairing channel, and practical calculations must resort to phenomenological regularization procedures [8]. Moreover, approaches based on the effective density-functional theory allow terms to be present in the functional, that do not originate from a two-body Hamiltonian. The price to pay is the occurrence of divergences when going beyond mean-field and restoring the particle number [9, 10]. These difficulties do not ex-

ist when finite-range effective interactions are used [9]. However, as of today, the description of weakly-bound nuclei in the framework of finite-range mean-field theory was not available, as existing codes did not take into account continuum effects.

In this paper, we present the first attempt to extend the mean-field approach based on finite-range interactions of the Gogny type to weakly-bound nuclei, by simultaneously taking into account continuum effects and the particle number symmetry. In section I we describe our method, which relies on the expansion of the mean-field solutions on a realistic basis. In section II is shown a selection of results benchmarking our method and illustrating the influence of the continuum in weakly-bound nuclei calculations. Projection on good particle number is discussed in section III.

I. FINITE-RANGE MEAN-FIELD THEORIES WITH COUPLING TO THE CONTINUUM

Mean-field calculations with finite-range interactions are most conveniently carried out in configuration space. In the HFB theory quasi-particle wave-functions are thus expanded on a basis of well-known functions. In nuclear structure, the harmonic oscillator basis has always played a special role, as it produces localized eigenstates that are known analytically. However, a well-known deficiency of this basis is its improper asymptotic behavior. While continuum states are spherical waves and therefore decay exponentially, HO functions behave like Gaussian functions. Unless the number of basis functions is prohibitively large, it is therefore impossible to describe all features of weakly-bound nuclei with such basis states.

Apart from the techniques already mentioned [3, 4, 5, 6], one simple and elegant way to overcome this problem is to use the eigenstates of a "realistic" nuclear potential, that is, of a potential that tends to 0 at infinity. Such a

potential generates both a sequence of strongly localized bound-states and of unlocalized positive-energy states. In practical calculations, boundary conditions must be set. Outgoing wave boundary conditions with wave number k assure that all solutions with positive energy are taken into account (within the indispensable discretization of the k values in practical numerical calculations), including resonant and non-resonant states. However, the wave-functions are not square-integrable, and special techniques must be employed to introduce the completeness relation and calculate the matrix elements of the interaction on such a basis [11, 12, 13, 14]. On the other hand, vanishing boundary conditions, alternatively named box boundary conditions, boil down to selecting only those positive-energy states that have a node on the boundaries of the domain of integration. Consequently, not the full continuum is taken into account, but the wave-functions are orthonormal. For nuclear structure applications and the description of ground-state properties the box technique is sufficient and in fact equivalent to the full continuum [15].

Our model potential was of the Woods-Saxon type, which reads in spherical symmetry:

$$V(r) = -\frac{V_0}{1 + \exp[(r - r_0)/a_0]} \quad (1)$$

The analytical solutions to the Schrödinger equation with this potential are not known apart from s-waves states [16]. However, they can be determined easily by well-established numerical integration methods. We enclose the potential in a sphere of radius R_{box} , discretize the space with a mesh size h and integrate the radial Schrödinger equation numerically:

$$\frac{d^2 y_{n\ell}}{dr^2} + \frac{2m}{\hbar^2} \left[e_{n\ell} - \frac{\ell(\ell+1)}{2mr^2} - V(r) \right] y_{n\ell}(r) = 0 \quad (2)$$

Our tests showed that a mesh size of $h \sim 0.1$ fm guaranteed the convergence of the subsequent HFB calculation to within a few keV.

The parameters of the potential do not play a major role here, as the eigenfunctions are only used as a basis. Therefore, the particular form of the Woods-Saxon potential can only affect the speed at which convergence is reached but not the final HFB result. We noticed that in order to obtain a fast convergence across the whole mass table, the potential should contain a consequent amount of bound-states. We therefore adopted the following parameters, that correspond to a realistic parametrization of the nuclear mean-field of element $Z = 126$ [17]: $V_0 = -41.619$ MeV, $r_0 = 1.000$ fm, $a_0 = 1.693$ fm.

Of more importance is the cut-off of the basis. Like in every numerical implementation of the mean-field theory, the basis can not be infinite but must be limited artificially. In practice, our basis functions are characterized by two quantum numbers, ℓ and n . Contrary to the harmonic oscillator basis, where the main shell number N provides a convenient and physical cut-off criterion, in

the case of the most general potential, the existence of such a simple criterion can not be guaranteed. Numerical tests showed that in heavy nuclei, $\ell_{max} = 15$ and $n_{max} = 18$ allowed very accurate calculations from drip-line to drip-line to within 10 keV. For the same required accuracy, calculations performed with an energy cut-off (all basis states with eigenvalues lower than E_{cut} are retained) reached convergence for E_{cut} of the order of 400 MeV. About 92% of such a basis is made of positive-energy unlocalized continuum states.

The Gogny interaction is a finite-range force that contain a central or Brink-Boeker term, a spin-orbit, density-dependent and Coulomb terms. The spin-orbit and Coulomb terms are the same as for zero-range Skyrme forces [18]. Only a few parametrizations of this interaction exist. All of our calculations were carried out with the D1S force [19]. We will study in a forthcoming paper the behavior of the isovector part of the Gogny interaction in the region of the neutron-drip-line.

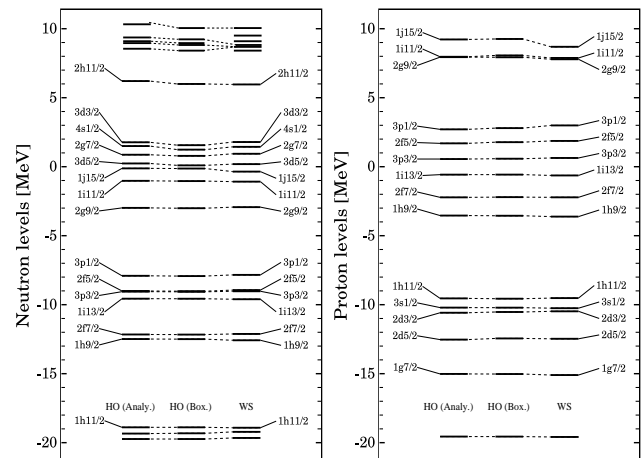


FIG. 1: Neutron (left) and proton (right) single-particle energies in ^{208}Pb calculated in the Hartree-Fock approach with the D1S Gogny effective interaction ($\ell_{max} = 15$ and $n_{max} = 18$). The first two columns in each figure correspond to the harmonic oscillator basis with $N = 24$ shells, with either Gauss-Hermite ('Analy.') or numerical ('Box.') integrations. The column on the right corresponds to the Woods-Saxon basis.

Figure 1 shows the single-particle spectrum in ^{208}Pb around the Fermi level as function of the type of basis used for the calculation. Benchmark calculations were performed in the HO basis using standard Gauss-Hermite quadrature formulas for the integrations (left column) [20]. The middle column shows the results when the HO basis wave-functions are obtained by integrating the Schrödinger equation for a HO potential in a box and using numerical integration techniques to compute the matrix elements of the Gogny interaction. Results obtained in the WS basis are shown in the column on the right. As required, all three calculations give nearly identical results for bound-states, within the numerical accuracy of the integration.

Let us notice that, as the convergence in the HO basis depends on the number of shells and of the oscillator length, the convergence in the WS basis depends on the cut-offs ℓ_{max} and n_{max} (or alternatively E_{cut}), on the parameters of the WS potential itself *and* on the size of the box. A detailed study of the convergence properties of the WS basis will be presented elsewhere.

TABLE I: Table of Fermi level and separation energies in drip-line nuclei

Neutrons			Protons		
	λ_n	$-S_{2n}$		λ_p	$-S_{2p}$
²⁰ C	-1.39	2.92	¹⁰ C	-3.78	11.78
²⁶ O	-0.36	1.16	¹⁴ O	-4.84	11.96
³⁰ Ne	-0.88	3.78	¹⁸ Ne	-2.38	5.18
⁴⁰ Mg	-0.47	1.44	²⁰ Mg	-1.09	2.66
⁴⁶ Si	-0.43	1.50	²⁴ Si	-2.06	6.24
⁵⁰ S	-0.17	1.30	²⁸ S	-1.20	5.22
⁵⁶ Ar	-0.59	1.46	³² Ar	-1.46	4.18
⁶⁴ Ca	-0.09	0.06	³⁶ Ca	-1.01	5.56
⁷² Ti	-0.18	0.66	⁴⁰ Ti	-0.27	1.78
⁷⁶ Cr	-0.16	0.62	⁴⁴ Cr	-1.21	3.24
⁸² Fe	-0.26	0.86	⁴⁶ Fe	-0.17	1.02
⁸⁶ Ni	-0.22	0.98	⁵² Ni	-1.18	5.41
⁹² Zn	-0.18	0.60	⁵⁸ Zn	-0.70	2.53
¹⁰⁴ Ge	-0.12	0.14	⁶² Ge	-0.77	3.22
¹¹⁴ Se	-0.33	0.76	⁶⁶ Se	-0.89	3.54
¹¹⁶ Kr	-1.10	2.24	⁶⁸ Kr	-0.08	0.71
¹²⁰ Sr	-0.44	2.76	⁷² Sr	-0.54	1.88
¹²² Zr	-1.02	4.36	⁷⁸ Zr	-1.12	3.37
¹³⁰ Mo	-0.02	0.16	⁸² Mo	-0.38	2.90
¹³⁶ Ru	-0.01	0.14	⁸⁶ Ru	-0.63	2.12
¹⁴⁰ Pd	-0.08	0.42	⁹⁰ Pd	-0.86	2.45
¹⁵² Cd	-0.03	0.04	⁹⁴ Cd	-1.05	2.66
¹⁷⁰ Sn	-0.03	0.12	¹⁰² Sn	-0.70	6.06
¹⁷⁶ Te	-0.44	0.90	¹¹⁰ Te	-0.04	1.53
¹⁷⁸ Xe	-0.99	1.98	¹¹⁴ Xe	-0.19	1.43
¹⁸⁰ Ba	-1.51	3.02	¹¹⁸ Ba	-0.37	1.62
¹⁸⁴ Ce	-0.26	3.16	¹²² Ce	-0.50	1.80
¹⁸⁶ Nd	-0.65	4.10	¹²⁶ Nd	-0.52	1.79
¹⁸⁸ Sm	-1.08	5.06	¹³⁰ Sm	-0.41	1.59
¹⁹⁰ Gd	-1.52	6.00	¹³⁴ Gd	-0.04	1.32
¹⁹⁸ Dy	-0.10	0.38	¹⁴⁰ Dy	-0.34	1.39
²⁰⁶ Er	-0.02	0.04	¹⁴⁴ Er	-0.19	1.14
²²⁰ Yb	-0.02	0.02	¹⁴⁸ Yb	-0.11	0.90
²⁴⁰ Hf	-0.03	0.12	¹⁵² Hf	-0.05	0.72
²⁵² W	-0.06	0.20	¹⁵⁸ W	-0.59	1.76
²⁵⁸ Os	-0.15	0.32	¹⁶² Os	-0.49	1.48
²⁶⁰ Pt	-0.44	0.88	¹⁶⁶ Pt	-0.38	1.17
²⁶² Hg	-0.71	1.42	¹⁷⁰ Hg	-0.25	0.79
²⁶⁴ Pb	-1.00	1.46	¹⁸² Pb	-0.08	4.12
²⁶⁸ Po	-0.00	1.70	¹⁹⁴ Po	-0.16	1.84
²⁷⁰ Rn	-0.24	2.22	¹⁹⁸ Rn	-0.07	1.11
²⁷² Ra	-0.50	2.72	²⁰⁴ Ra	-0.43	1.70
²⁷⁴ Th	-0.76	3.22	²⁰⁸ Th	-0.21	1.26
²⁷⁶ U	-1.04	3.76	²¹⁴ U	-0.32	1.56
²⁸² Pu	-0.06	0.28	²²⁰ Pu	-0.42	1.54
²⁹⁶ Cm	-0.04	0.04	²²² Cm	-0.17	1.11

II. DRIP-LINES AND CONTINUUM EFFECTS

As an application of the consideration of continuum effects in practical calculations we present in Table I the neutron and proton drip-lines calculated in the spherical HFB approach for the Woods-Saxon basis. For the listed elements, the two-neutrons S_{2n} and two-protons S_{2p} separation energies were calculated, as well as the position of the Fermi level. The criterion to define the drip-line was either a positive separation energy, or a positive Fermi level, whichever criterion was met first. The WS basis included all states with $\ell \leq 15$ and $n \leq 18$ in a box of $R_{box} = 20$ fm.

Drip-lines can be significantly pushed away by long-range correlations. In particular, rare-earth nuclei are found to be strongly deformed either in large-scale Gogny HFB calculations using the D1S interaction [21] and including beyond mean-field correlations [22] as well as in Skyrme HFB calculations performed in the transformed harmonic oscillator basis with the SLy4 parametrization in the mean-field channel and the volume delta pairing force [23]. Bearing this fact in mind, we nevertheless observe systematic differences on the position of the neutron drip-line as compared to Skyrme HFB calculations published in [23] where the drip-line almost systematically extends further away by 2-4 neutrons.

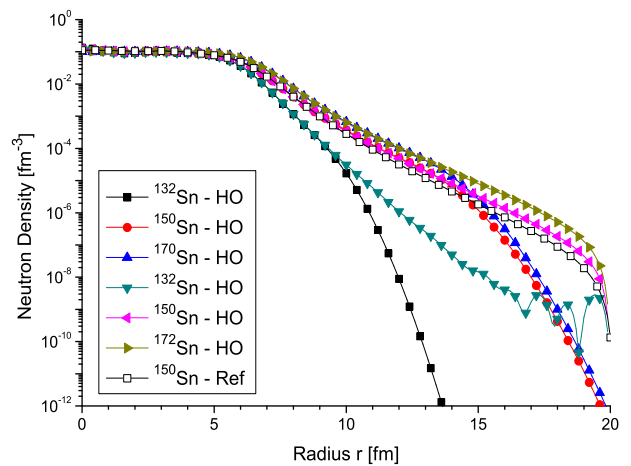


FIG. 2: (color online) Neutron densities in neutron-rich ^{132,150,170}Sn isotopes computed with the finite range D1S Gogny interaction in the HO and Woods-Saxon bases for a box of 20 fm. The curve marked Ref. is the HFB calculation in coordinate space for ¹⁵⁰Sn with the SkP force [3]. The unphysical asymptotic behavior of densities computed in the HO basis is clearly visible. Oscillations in the case of ¹³²Sn are caused by the absence of pairing correlations which forbids ℓ -couplings in the expansion.

Observables like densities are very sensitive to continuum effects and significantly impact many spectroscopic or reaction properties of nuclei. A stringent test of our

method is therefore its ability to reproduce the long tails of neutron densities in neutron-rich nuclei. There have been numerous studies of neutron skins in exotic nuclei in the past, and we can therefore benchmark our approach.

As an example we display in figure 2, the neutron densities of three very neutron-rich Sn isotopes. For small and medium values of the nuclear radius the HO and the WS bases give the same density profile. However, for large radius the differences are significant. As expected, the proper asymptotic of the WS basis wave-functions is reflected in the long density tails. It is important to emphasize that the results are nearly identical to coordinate space Skyrme HFB calculations of [3] as can be seen from the curve marked Ref., which shows the density in ^{150}Sn obtained with the SkP parametrization of the Skyrme interaction. This provides an independent validation and very robust test of our method to incorporate continuum effects through a basis.

We observe oscillations in the densities for closed-shell nuclei like ^{132}Sn . Indeed, in that case the density is simply the sum of N well-localized single-particle states, and no contribution from discretized continuum states enters the expansion. The threshold where these oscillations appear gives in fact a measure of the intrinsic numerical accuracy with which integrations are performed. This phenomenon may be distinguished from what was reported in [24] where oscillations were caused by large discrepancies between the upper and lower components in the HFB equations.

III. RESTORATION OF THE PARTICLE NUMBER SYMMETRY

As mentioned in the introduction pairing correlations play a relevant role in the description of weakly bound nuclei. Up to now most descriptions of the drip-line were performed in the HFB approach which has two drawbacks. Firstly, in the weak pairing regime it usually collapses to the unpaired solution and secondly, the HFB wave function has the right number of particles only on the average. To restore this spontaneously broken symmetry, we project the HFB solution onto good particle number using the projector:

$$\hat{P}^N = \frac{1}{2\pi} \int_0^{2\pi} d\varphi e^{i\varphi(\hat{N}-N)} \quad (3)$$

according to the procedure described in details in [9]. As is well-known, the variation after projection (VAP) method provides a much better approach than the projection after variation (PAV) at the cost of a much higher numerical effort, especially with the huge basis used in the present calculations. In particular, it prevents pairing correlations to collapse. Nevertheless one can obtain an approximate VAP solution by searching for the minimum in a restricted highly pair-correlated variational space [25]. This space is generated by HFB solutions

$|\phi(x)\rangle$ corresponding to the self-consistent diagonalization of the one-body Hamiltonians $\hat{h}_{HFB}(x)$, as a function of x . Here $\hat{h}_{HFB}(x)$ stands for the HFB Hamiltonian obtained by multiplying, at each iteration, the pairing field Δ of the HFB matrix by the constant x , i.e., $\Delta \rightarrow \Delta(x) = x\Delta$, while the particle-hole field h remains unchanged. To each wave function $|\phi(x)\rangle$ is associated an eigenstate of the particle number operator $|\Phi(x)\rangle = \hat{P}^N|\phi(x)\rangle$ and an energy

$$E^N(x) = \frac{\langle\Phi(x)|\hat{H}|\Phi(x)\rangle}{\langle\Phi(x)|\Phi(x)\rangle} \quad (4)$$

with \hat{H} the *original* two-body Hamiltonian. The variational principle guarantees that such a procedure yields a minimum as function of x , which is an excellent approximation to the VAP result [25]. We call this approach RVAP (Restricted VAP).

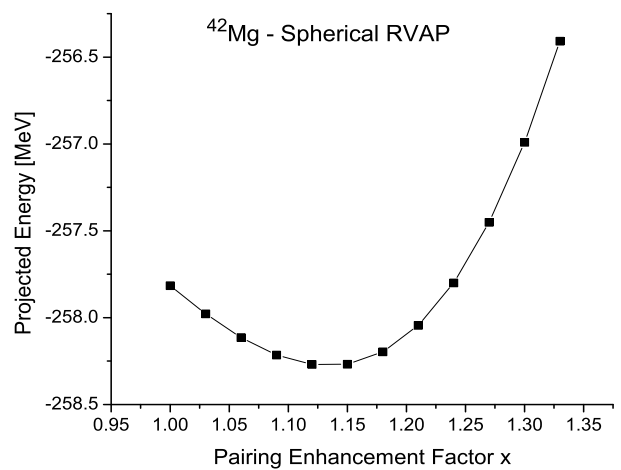


FIG. 3: (color online) Total projected energy $E^N(x)$ in ^{42}Mg as function of the effective pairing strength factor x . The RVAP calculation was performed in the WS basis.

To investigate the impact of a better treatment of pairing correlations on exotic nuclei we applied this restricted VAP procedure in the neighborhood of the neutron drip-line. Figure 3 shows the example of ^{42}Mg which is unbound against 2 neutrons emission in standard spherical HFB or PAV-HFB calculations. The minimum of the curve depicted in Fig. 3 corresponds to a stronger pairing regime than in standard HFB calculations: the total gain in energy is only 460 keV but the pairing energy goes from -9.22 MeV to -13.83 MeV from $x = 1.0$ to $x = 1.12$. At the minimum, the two-neutron separation energy calculated from the RVAP projected energies of ^{42}Mg and ^{40}Mg becomes negative at $S_{2n} = -252$ keV (compared with $S_{2n} = +40$ keV in the un-projected case) and the nucleus is bound against 2 neutrons emission. This effect is usually typical from nuclei near closed-shells where only the VAP method can prevent the HFB theory to col-

lapse to the unpaired regime. Near the drip-lines, it also results in a visible shift of the drip-lines. It is important to realize that this effect can not appear in a PAV calculation.

The restoration of symmetries broken at the mean-field level has therefore a significant and experimentally visible effect in exotic neutron-rich nuclei. Variation after projection on good particle number consists in exploring a different variational space than when the projection is carried out after the variation.

In summary, we present the first results of a generalization of HFB calculations with finite-range interactions to exotic weakly-bound nuclei. Mean-field solutions are expanded on a basis of the eigenstates of a Woods-Saxon potential, which possess the proper asymptotic behavior. In stable nuclei, this WS basis is benchmarked against standard harmonic oscillator calculations and is found to give exactly the same results. In neutron-rich nuclei

we find that the asymptotic of the neutron densities is properly reproduced. The role of the restoration of particle number *before variation* is emphasized. It is found that this mechanism can stabilize nuclei at the drip-line thereby pushing away the latter.

Acknowledgment - We wish to thank P. Ring and T. R. Rodriguez for fruitful discussions. One of us (N.S.) acknowledges financial support of the spanish Ministerio de Educacion y Ciencia (Ref. SB2004-0024). This work has been supported in part by the DGI, Ministerio de Ciencia y Tecnologia, Spain, under Project FIS2004-06697, as well as by the U.S. Department of Energy under Contract Nos. DE-FC02-07ER41457 (University of Washington), DEFG02-96ER40963 (University of Tennessee), and DE-AC05-00OR22725 with UT-Battelle, LLC (Oak Ridge National Laboratory). We thank K. Bennaceur and J. Dobaczewski for letting us use the code HFBRAD.

-
- [1] J. Dobaczewski and W. Nazarewicz Phil. Trans. R. Soc. Lond. A **356**, 2007-2031 (1998)
- [2] J. Dobaczewski, N. Michel, W. Nazarewicz, M. Płoszajczak and J. Rotureau Prog. Part. Nucl. Phys. **56**, 432-455 (2007)
- [3] J. Dobaczewski, H. Flocard and J. Treiner, Nucl. Phys. **A422**, 103 (1984); J. Dobaczewski, W. Nazarewicz, T. R. Werner, J.-F. Berger, C. R. Chinn and J. Dechargé, Phys. Rev. **C53**, 2809-2840 (1996)
- [4] M. V. Stoitsov, W. Nazarewicz and S. Pittel, Phys. Rev. **C58**, 2092 (1998); M. V. Stoitsov, J. Dobaczewski, W. Nazarewicz and P. Ring, Comput. Phys. Commun. **167**, 43-63 (2005)
- [5] M. Grasso, N. Sandulescu, N. Van Giai and R. J. Liotta, Phys. Rev. **C64**, 064321 (2001)
- [6] W. Poeschl, D. Vretenar and P. Ring, Comp. Phys. Comm. **103**, 217 (1997)
- [7] N. Michel, W. Nazarewicz, M. Płoszajczak and J. Okolowicz Phys. Rev. **C67**, 054311 (2003); N. Michel, W. Nazarewicz, M. Płoszajczak and K. Bennaceur Phys. Rev. Lett. **89**, 042502 (2002)
- [8] P. Borycki, J. Dobaczewski, W. Nazarewicz and M. Stoitsov Phys. Rev. **C73**, 044319 (2006)
- [9] M. Anguiano, J.L. Egido and L.M. Robledo Nucl.Phys. **A696**, 467-493 (2001); M. Anguiano, J.L. Egido and L.M. Robledo Phys. Lett. **B545**, 62-72 (2002);
- [10] J. Dobaczewski, M.V. Stoitsov, W. Nazarewicz, P.-G. Reinhard, nucl-th/arXiv:0708.0441
- [11] Y.B. Zel'dovich, Sov. Phys. JETP. **12**, 542 (1960); N. Hokkyo, Prog. Theor. Phys. **33**, 1116 (1965); W. J. Romo, Nucl. Phys. **A116**, 617 (1968);
- [12] T. Berggren, Nucl. Phys. **A109**, 265 (1968);
- [13] B. Gyarmati and T. Vertse, Nucl. Phys. **A160**, 523 (1971); G. Garcia-Calderon and R. Peierls, Nucl. Phys. **A265**, 443 (1976);
- [14] P. Lind, Phys. Rev. **C47** 1903 (1993)
- [15] M. Stoitsov, N. Michel and K. Matsuyanagi, nucl-th/arXiv:0709.1006
- [16] S. Flügge, Practical Quantum Mechanics I (Springer-Verlag, Berlin, 1971) vol. 1, Prob. No. 37, 39.
- [17] J. Dudek and T. R. Werner, Phys. Lett. **10**, 1543 (1978)
- [18] J. Dechargé and D. Gogny, Phys. Rev. **C21**, 1568 (1980)
- [19] J.-F. Berger, M. Girod and D. Gogny, Comput. Phys. Commun. **63**, 365 (1991)
- [20] T. Gonzalez-Llarena, Ph.D Thesis, Universidad Autonoma de Madrid, Sep. 1999, unpublished.
- [21] http://www-phynu.cea.fr/science_en_ligne/carte_potentiels_microscopiques/carte_potentiel_nucleaire.htm
- [22] T. R. Rodriguez and J. L. Egido, Phys. Rev. Lett. **99**, 062501 (2007)
- [23] M. V. Stoitsov, J. Dobaczewski, W. Nazarewicz, S. Pittel and D. J. Dean, Phys. Rev. **C68**, 054312 (2003)
- [24] K. Bennaceur and J. Dobaczewski, Comp. Phys. Comm. **168**, 96-122 (2005)
- [25] T. R. Rodriguez, J. L. Egido and L. M. Robledo, Phys. Rev. **C72**, 064303 (2005)